Detection and characterization of corrosion of bridge cables by time domain reflectometry

Wei Liu [*a], Robert Hunsperger[a], Kevin Folliard[b], Michael Chajes[b],

Jignesh Barot[b], Darshan Jhaveri[b], Eric Kunz[c]

[a]Dept. of Electrical & Computer Engineering, Univ. of Delaware, Newark, DE 19716

[b]Dept. of Civil & Environmental Engineering, Univ. of Delaware, Newark, DE 19716

[c]VETEK Systems Corp. 6 Oak Road, Elkton, MD 21921

ABSTRACT

In this paper, we develop and demonstrate a nondestructive evaluation technique for corrosion detection of embedded or encased steel cables. This technique utilizes time domain reflectometry (TDR), which has been traditionally used to detect electrical discontinuities in transmission lines. By applying a sensor wire along with the bridge cable, we can model the cable as an asymmetric, twin-conductor transmission line. Physical defects of the bridge cable will change the electromagnetic properties of the line and can be detected by TDR. Furthermore, different types of defects can be modeled analytically, and identified using TDR. TDR measurement results from several fabricated bridge cable sections with built-in defects are reported.

Keywords: Corrosion detection, Nondestructive evaluation, TDR

1. INTRODUCTION

The corrosion of metallic reinforcement is a major threat to aging infrastructure. The high-strength steel used for the cables of suspension and cable-stayed bridges is very sensitive to corrosion, and failure of cables is a serious problem due to the limited degree of redundancy in the structure. While visual inspection is the most effective method of corrosion detection in some instances, it can not be used for embedded or encased steel cables. A reliable, accurate, and economical method for detecting the location and magnitude of the corrosion is urgently needed.

Several indirect nondestructive corrosion detection methods have been developed. They can be grouped into two main categories: mechanical methods and electromagnetic methods. Mechanical methods use force measurement. The tension force in a bridge cable is measured either directly by pulling on the cable or indirectly by observing its free damped vibrations. The vibration frequency reveals the tension in the cable. Although these mechanical tests are easy to apply, they have two main disadvantages: they can not pinpoint the location of the damage, and they are relatively insensitive. Furthermore, force measurement methods can only be used for certain types of cables.

The simplest electrical method is resistance measurement. It measures the end-to-end ohmic resistance of the steel cable. Any reduction of cross-sectional area due to corrosion will cause an increase in the resistance. The location of the corrosion can not be detected by this measurement. As might be expected, this method is very sensitive to temperature variations in the environment.

Another corrosion monitoring method, potential field measurement, is based on the electrochemical reaction due to active corrosion. In this method, a silver wire running parallel to the cable is embedded during fabrication in the concrete grout surrounding the steel cable. Active corrosion will cause an increase in the electrical potential between the silver wire and the steel cable, typically from 150mV to about 400mV.[1] This voltage change can be easily detected. However, this method can neither pinpoint the location of corrosion, nor detect the extent or magnitude of corrosion that has occurred.

A more accurate electromagnetic method uses magnetic inductance scanning.[2] In this method, a strong magnetic field is generated around the steel cable. Corrosion pits, which change the boundary conditions of the field, will cause a field disturbance and therefore can be detected. This method is expensive, complicated, and time-consuming to

[*]Correspondence: Email: wliu@ee.udel.edu; Telephone: (302) 831-6693; Fax: (302) 831-4316

employ since it scans the cable section by section. In order to produce the magnetic field, heavy devices are necessary. This makes the method awkward to use for many structures.

In this paper, we develop and demonstrate a nondestructive evaluation technique using time domain reflectometry (TDR). This method of corrosion detection is superior to these previous methods in that it can detect, locate and identify the extent of corrosion.

TDR has traditionally been used in the field of electrical engineering to detect discontinuities in a transmission line. It involves sending an electrical pulse along the transmission line and using an oscilloscope to observe the echoes. Any discontinuity will cause a reflection. From the transit time, magnitude, and polarity of the reflection, it is possible to determine the spatial location and nature of the discontinuity. One can model the bridge cable as an asymmetric, twin-conductor transmission line by applying a sensor wire along with the cable. Physical defects of the bridge cable, such as abrupt pitting corrosion, general surface corrosion, and voids in the concrete grout, will change the electromagnetic properties of the line. These defects, which can be modeled as different kinds of discontinuities, can be detected by TDR.

2. TRANSMISSION LINE AND TIME DOMAIN REFLECTOMETRY

2.1. A Brief Introduction to Transmission Line Theory

A transmission line is a kind of waveguiding system. It usually consists of two or more parallel conductors. For a through analysis of the wave propagation in a transmission line, one needs to solve Maxwell's equations with boundary conditions imposed by the physical nature of the system under investigation. It is also possible to represent a line by the distributed parameter equivalent circuit and discuss wave propagation in terms of voltage and current.

The distributed parameter equivalent circuit of a transmission line is shown in Figure 1. It possesses a uniformly distributed series resistance $\mathcal{R}$, series inductance $\mathcal{L}$, shunt capacitance $\mathcal{C}$, and shunt conductance $\mathcal{G}$.* By studying this equivalent circuit, several characteristics of the transmission line can be determined.

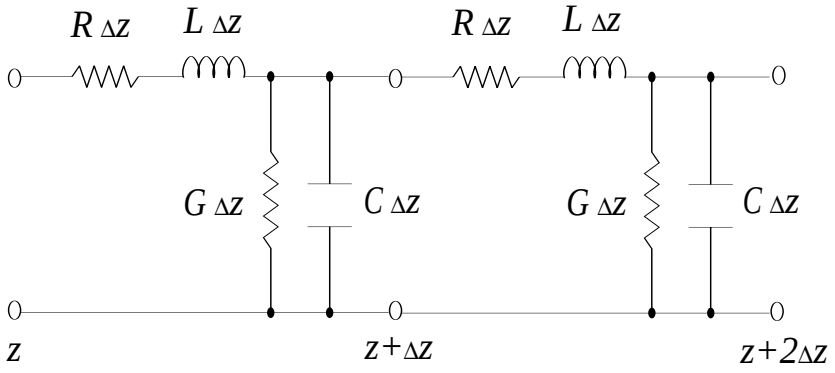

Figure 1. Distributed parameter equivalent circuit of a transmission line

The transmission line equations can be obtained by applying Kirchhoff's voltage and current laws to the distributed equivalent circuit. They are given by

$$\frac{\partial v}{\partial z} = -(\mathcal{R}i + \mathcal{L}\frac{\partial i}{\partial t}) \quad (1)$$

$$\frac{\partial i}{\partial z} = -(\mathcal{G}v + \mathcal{C}\frac{\partial v}{\partial t}) \quad (2)$$

in which v and i are the instantaneous values of the line voltage and current at an arbitrary point z. They are functions of time t and position z. Suppose them to be given by $Ve^{j\omega t}$ and $Ie^{j\omega t}$ respectively, with V and I being the amplitudes of the voltage and current at the point z. Making these substitutions and eliminating I we get

$$\frac{\partial^2 V}{\partial z^2} = (\mathcal{R} + j\omega\mathcal{L})(\mathcal{G} + j\omega\mathcal{C})V = \gamma^2 V$$

*$\mathcal{R}$, $\mathcal{L}$, $\mathcal{C}$, and $\mathcal{G}$ are defined per unit length.

where

$$\gamma = \alpha + j\beta = \sqrt{(\mathcal{R} + j\omega\mathcal{L})(\mathcal{G} + j\omega\mathcal{C})} \tag{3}$$

and γ is the propagation constant, it defines the phase shift (β) and attenuation (α) per unit length. The velocity at which the voltage travels down the line can be defined in terms of β:

$$v_p = \frac{\omega}{\beta} \tag{4}$$

V and I are related by

$$I = \frac{V}{Z_0}$$

where Z_0 is the characteristic impedance of the line. It is given by

$$Z_0 = \sqrt{\frac{\mathcal{R} + j\omega\mathcal{L}}{\mathcal{G} + j\omega\mathcal{C}}} \tag{5}$$

At every point that the excitation signal crosses, the transmission line equations must be obeyed. For a line terminated by a load Z_l, if Z_l is different from Z_0, the transmission line equations are not satisfied unless a second wave is considered to originate at the load and to propagate back up the line, i.e., a reflection is generated at this point. The ratio of reflected voltage to the incident voltage is defined as voltage reflection coefficient, ρ, and is related to Z_l and Z_0 by the equation

$$\rho = \frac{V_r}{V_i} = \frac{Z_l - Z_0}{Z_l + Z_0} \tag{6}$$

2.2. Time Domain Reflectometry

Time Domain Reflectometry (TDR) is an electrical measurement technique that has been used since the 1940s to determine the spatial location and nature of various objects. It involves sending an electrical pulse along a transmission line and using an oscilloscope to observe the echoes returning back from the device under test.

A time domain reflectometer is usually configured as shown in Figure 2. The pulse generator generates a fast rising step wave or pulse. This wave is launched into the transmission line. A high impedance oscilloscope is connected through a tee adapter to monitor the wave.

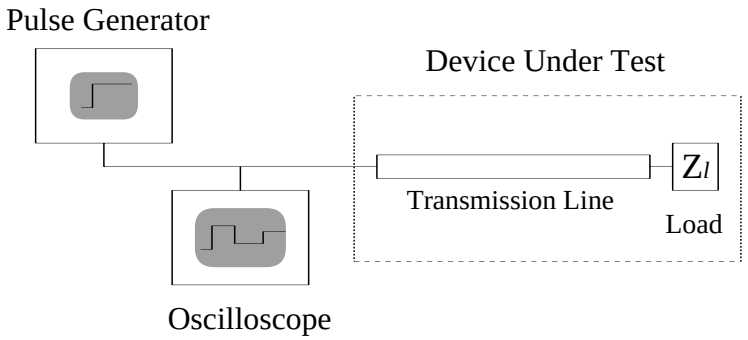

Figure 2. Functional block diagram for a typical time domain reflectometer

2.2.1. Locating mismatches and analyzing reflections

An examination of the time delay and wave shape of the echoes allows us to determine the location and nature of discontinuities within the transmission line.

The wave travels down the transmission line at the velocity of propagation of the line, v_p. If a mismatch exists in the line, part of the incident wave is reflected. The reflected wave is separated in time from the incident wave. This

time, T, is the transit time from monitoring point to the mismatch and back again, as measured on the oscilloscope. The distance from the monitoring point to the mismatch is given by

$$D = \frac{v_p T}{2} \tag{7}$$

The velocity of propagation can be determined either from an experiment on a known length of the same type of cable or from theoretical calculation using equation (4).

The shape of the reflected wave reveals both the nature and magnitude of the mismatch. Assume that the excitation signal is step function wave. A pure resistive load Z_l will reflect a voltage of the same shape as the driving voltage, with the magnitude and polarity determined by the relative values of Z_l and Z_0. TDR returns from pure resistive loads are illustrated in Figure 3 in plots of measured voltage versus time. We can measure the reflected voltage V_r and the incident voltage V_i and calculate the voltage reflection coefficient ρ. From equation (6),

$$Z_l = \frac{1+\rho}{1-\rho} Z_0 \tag{8}$$

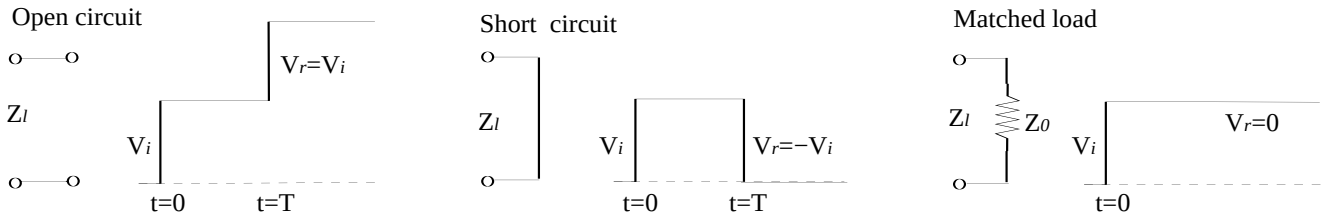

Figure 3. TDR Returns from Pure Resistive Loads

2.2.2. Reactive loads

Reactive components, inductance (L) and capacitance (C), can also be measured using TDR. Four common cases of TDR reflections from reactive elements are shown in Figure 4.[3]

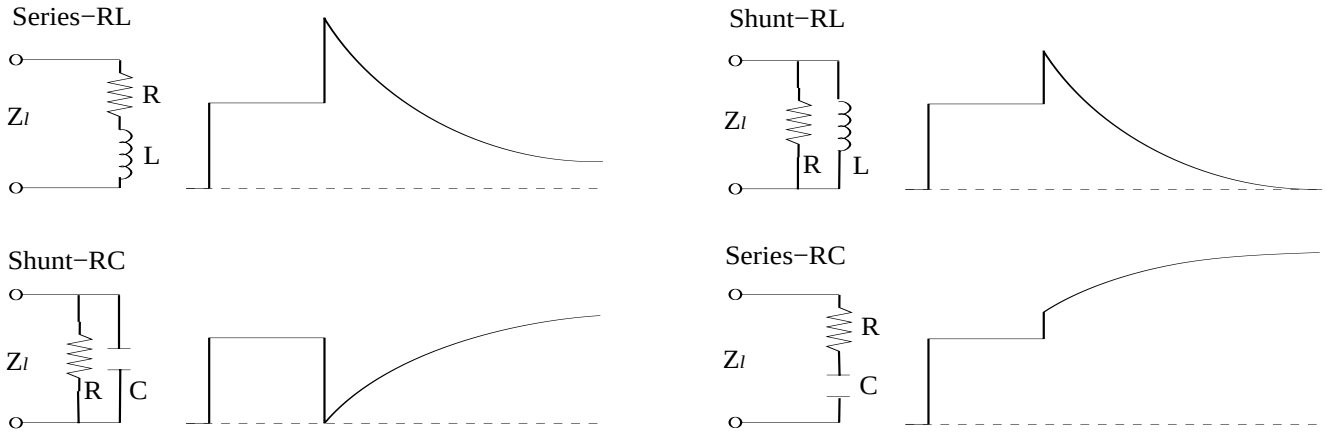

Figure 4. TDR returns from reactive loads

Theoretical analysis of the waveform can be accomplished by Laplace transform. If the impedance of the reactive load in the Laplace domain is $Z_l(s)$, then the reflection coefficient is given by

$$\rho(s) = \frac{Z_l(s) - Z_0}{Z_l(s) + Z_0} \tag{9}$$

assuming that Z_0 is real, i.e., pure resistive. The reflection from this load in the Laplace domain is then

$$V_r(s) = V_i(s)\ \rho(s) \tag{10}$$

By converting $V_r(s)$ back to the time domain, we obtain the expression of the reflected wave.

Another simpler analysis is also possible by simply considering the behavior of inductors and capacitors.[4] The inductor initially appears as an open circuit to the fast rising edge of the TDR step pulse, i.e., the high frequencies components of the wave. Later in time, the inductor appears as a short circuit to the flat top of the TDR step pulse, i.e., the DC portion. The capacitor performs exactly opposite. The L or C value may be determined by measuring the exponential time constant, τ, of the TDR response.

$$\tau = \frac{L}{R_{eff}} \quad or \quad \tau = CR_{eff} \tag{11}$$

where, R_{eff} is the effective resistance seen by the inductor or capacitor.

The TDR reflections shown in Figure 4 are the ideal situations in which the step wave has a risetime† of zero. With a finite risetime pulse generator and oscilloscope, these waveforms will no longer have sharp corners, but will have smooth rounded corners.

When the time constant associated with the reactive components is much greater than the system risetime T_r, i.e., the inductance or capacitance is large, we can suppose the system is perfect and has a zero risetime. The TDR return in this case will be very similar to the ideal TDR response. By measuring the time constant, τ, we can find out the value of the inductance or capacitance through equation (11).

When the time constant is of the same order of magnitude as the TDR system risetime, a different TDR return will be observed, as shown in Figure 5. It is merely a small peak with voltage V_{pk}. Equation (11) is not valid under this circumstance. However, L and C can still be calculated through some good empirical formulas.[5]

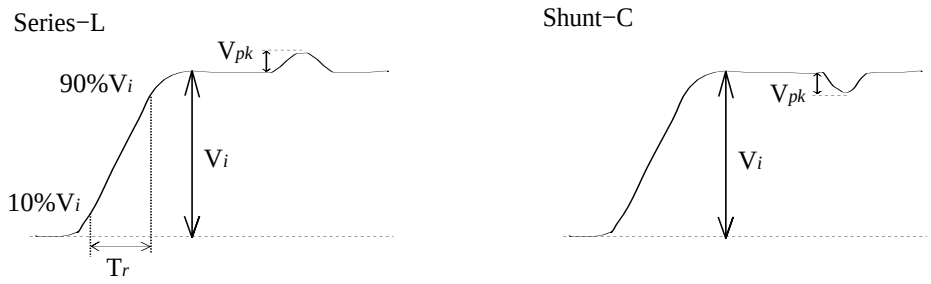

Figure 5. TDR displays of reactive loads from a TDR system with finite risetime, T_r, which is comparable to the time constant of the reactive components.

If the time constant of the reactive component is much less than the TDR system risetime, no visible reflections will occur. Therefore, small capacitors or inductors may not be measured unless a TDR system with shorter risetime is used.

2.2.3. Discontinuities at intermediate positions

Discontinuities at intermediate positions along the line can also be detected by TDR. The analysis of this kind of discontinuity is not much different from the analysis of the mismatched loads. When calculating the reflection coefficient, one needs to combine the impedance of the discontinuity and the impedance of the line after it to get the effective impedance at the point of mismatch. Another advantage of TDR is its ability to detect multiple discontinuities in a transmission line.

3. MODELING THE BRIDGE CABLE

TDR can be used to detect the location and severity of discontinuities in a transmission line. It is widely used not only in the field of electrical engineering, but also in some other fields such as geotechnical engineering and mining. TDR can also be effectively used to detect corrosion of bridge cables.[6]

By applying a sensor wire along with the bridge cable, we have the twin-conductor transmission line geometry, as shown in Figure 6. But there are still some important differences between this one and the classic transmission

† The risetime, T_r, is defined as the interval between the 10% and 90% amplitude points on the leading or trailing edge.

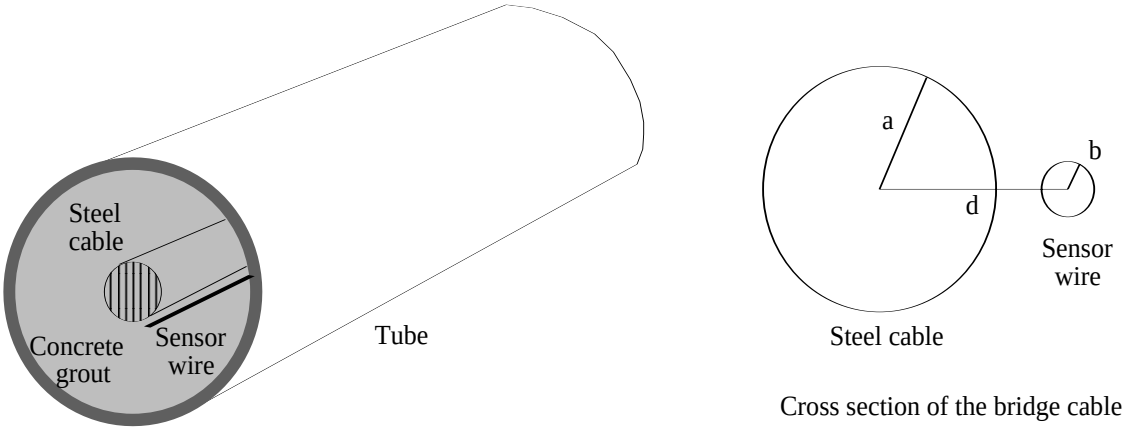

Figure 6. Twin-conductor transmission line geometry of a bridge cable with sensor wire, where a is the radius of the steel cable, b is the radius of the sensor wire, and d is the center-to-center distance between the cable and wire.

line. The two conductors have different diameters. They are embedded in concrete grout and encased in a tube; this imposes a complicated boundary condition. However, if the dimension of the concrete grout is much larger than the dimension of the steel cable and the sensor wire, we can assume these two conductors are in a uniform concrete medium, i.e., we neglect the influence of the tube. This simplification will not affect the analysis much because the electromagnetic field is concentrated between the two conductors and does not significantly extend through the grout to the tube.

3.1. Calculation of capacitance, inductance, resistance and conductance

It is desired to obtain the capacitance and inductance per unit length of the transmission line. Since we know the relationship between these two quantities, which is given by[7]

$$\mathcal{LC} = \mu\varepsilon \tag{12}$$

where μ and ε are the permeability and permittivity of the system, respectively, we only need to find the capacitance per unit length. The difficulty of our arrangement is that the two cylindrical conductors have different radii. We can do this by considering the electric field of two parallel infinitely long straight line charges of equal and opposite uniform charge densities. The equipotential surfaces are cylinders with axes parallel to the line charges. We know that if we place a perfectly conducting cylinder in any equipotential surface the electric field will not be disturbed. By placing the two conductors in two equipotential surfaces and calculating the potential difference, we obtain the capacitance per unit length of the line to be[8]

$$\mathcal{C} = \frac{2\pi\varepsilon}{\cosh^{-1}\left(\frac{d^2-a^2-b^2}{2ab}\right)} \tag{13}$$

and hence the inductance per unit length can be calculated by equation (12), which is

$$\mathcal{L} = \frac{\mu}{2\pi}\cosh^{-1}\left(\frac{d^2-a^2-b^2}{2ab}\right) \tag{14}$$

The resistance per unit length $\mathcal{R}$ has two parts, $\mathcal{R}_a$ and $\mathcal{R}_b$, which are the resistance of the bridge cable and sensor wire respectively. To calculate the resistance at high frequency, we must take skin effects into account. When the operating frequency is f, the skin depth is given by

$$\delta = \frac{1}{\sqrt{\pi f \mu \sigma}} \tag{15}$$

where, σ is the conductivity of the conductor.

The resistance of the transmission line is

$$\mathcal{R} = \mathcal{R}_a + \mathcal{R}_b = \sqrt{\frac{f\mu}{4\pi}}\,(\frac{1}{a\sqrt{\sigma_a}} + \frac{1}{b\sqrt{\sigma_b}}) \tag{16}$$

For concrete with low water content, the conductance is quite small. Additionally, there is an isolating layer of plastic insulation around the sensor wire. Therefore, the conductance $\mathcal{G}$ can be considered to be zero.

3.2. Characteristic impedance

According to equation (5), the characteristic impedance is given in terms of the quantities $\mathcal{C}$, $\mathcal{L}$, $\mathcal{R}$ and $\mathcal{G}$ by

$$Z_0 = \sqrt{\frac{\mathcal{R} + j\omega\mathcal{L}}{\mathcal{G} + j\omega\mathcal{C}}}$$

Since at very high frequencies $\mathcal{R}$ increases as $\sqrt{f}$, whereas $\omega\mathcal{L}$ increases directly as f, the ratio $\mathcal{R}/\omega\mathcal{L}$ decreases as $\sqrt{f}$.

$$\frac{\mathcal{R}}{\omega\mathcal{L}} = \frac{1}{\sqrt{4\pi\mu f}}\;\frac{\frac{1}{a\sqrt{\sigma_a}} + \frac{1}{b\sqrt{\sigma_b}}}{\cosh^{-1}(\frac{d^2-a^2-b^2}{2a\,b})}$$

Let us take $a = 0.635cm$, $b = 0.05cm$, and $d = 3.175cm$. At $f = 50MHz$, $\frac{\mathcal{R}}{\omega\mathcal{L}} = 1.08 \times 10^{-2}$, which is negligible compared with unity; it will clearly become still more negligible at higher frequencies. It has also been stated that $\frac{\mathcal{G}}{\omega\mathcal{C}}$ should desirably approximate to zero.

Under these circumstances the characteristic impedance is given to a high degree of accuracy by the simple expression

$$Z_0 = \sqrt{\frac{\mathcal{L}}{\mathcal{C}}} \tag{17}$$

On substituting for $\mathcal{C}$ and $\mathcal{L}$ from (13) and (14) the following expression for Z_0 results

$$Z_0 = \frac{1}{2\pi}\sqrt{\frac{\mu}{\varepsilon}}\cosh^{-1}(\frac{d^2-a^2-b^2}{2ab}) \tag{18}$$

This expression is entirely real, so that Z_0 has the character of a pure resistance.

3.3. Effect of small changes of dimensions

The characteristic impedance of the line is a function of a, b, and d. For the problem in which we are interested, b is much smaller than a and d, and it remains the same value along the line. However, the radius of the steel cable, a, may be changed if corrosion occurs. A plot of characteristic impedance Z_0 versus radius of bridge cable a is shown in Figure 7.

When $b \ll d$, we have

$$\begin{aligned}\frac{dZ_0}{da} &= -\frac{1}{2\pi}\sqrt{\frac{\mu}{\varepsilon}}\,\frac{1}{a}\,\frac{(d^2-b^2)+a^2}{\sqrt{(d^2-b^2)^2 - 2(d^2+b^2)a^2 + a^4}} \\ &\approx -\frac{1}{2\pi}\sqrt{\frac{\mu}{\varepsilon}}\,\frac{1}{a}\,\frac{d^2+a^2}{d^2-a^2}\end{aligned} \tag{19}$$

$\frac{dZ_0}{da}$ has a negative value. It means that the characteristic impedance will increase for a small decrease of a as shown in Figure 7. Since radius a always decreases at a corrosion site, corrosion will cause a higher characteristic impedance. This change of impedance can be detected by time domain reflectometry.

We also notice that $\frac{dZ_0}{da}$ depends on the value of $(d^2 - a^2)$. When the sensor wire is close to the steel cable, $(d^2 - a^2)$ is small, and $\frac{dZ_0}{da}$ is large. In this case, the characteristic impedance will have a greater change for the same decrease of a, and hence the TDR method will be more sensitive.

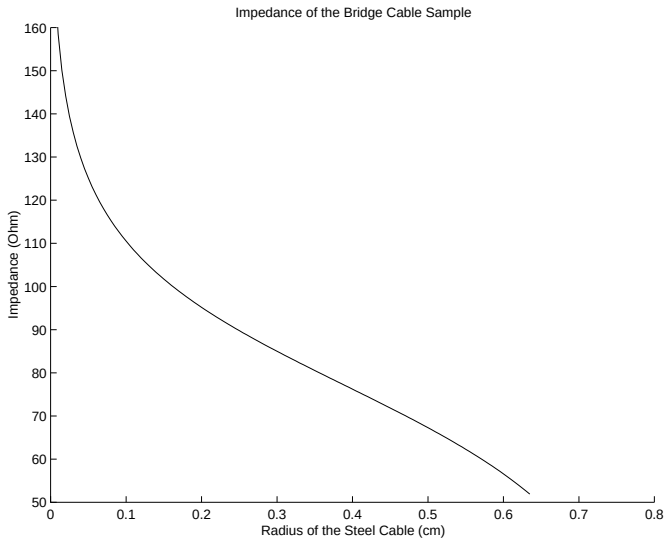

Figure 7. Characteristic impedance as a function of radius a, where $d = 0.800cm$, $b = 0.030cm$, and $a = 0.635cm$ if not corroded.

3.4. Modeling different types of corrosion

Several physical defects are of great interest when considering the durability of bridge cables. Among them are abrupt pitting corrosion, general surface corrosion, and voids in the concrete grout.

3.4.1. Pitting corrosion

Pitting corrosion is a serious defect characterized by severe localized damage. It greatly reduces the cross-sectional area of the steel cable. Since the characteristic impedance is a function of a, the radius of the steel cable, as shown in equation (18), the localized impedance should increase abruptly if pitting corrosion occurs. From the discussion of TDR in the previous section, we would expect a positive reflection from the site of pitting corrosion. The reflection coefficient can be measured from the reflected waveform. The impedance of the corrosion site can then be calculated from equation (6).

3.4.2. Surface corrosion

Surface corrosion tends to reduce the radius of the cable on the order of 1% to 5% over a length of the line. Although surface corrosion will also change the characteristic impedance, this change occurs gradually, so there is no large reflection on the TDR return. However, such a gradual change of impedance will cause an energy loss. Using a step wave, we can measure the energy loss per unit length by measuring the change of the step voltage. Detection of a greater loss over a certain part of the cable indicates that surface corrosion may be present.

3.4.3. Void in concrete grout

Although a void in the concrete grout will not change the strength of the reinforcing cable, it leaves a section of the cable vulnerable to corrosion. From equation (18), we can see that the characteristic impedance also depends on ε, which is the dielectric constant of the system. A void in the concrete will change this dielectric constant since the contents of the void, usually air and some water, have different electrical properties. Voids tend to reduce the dielectric constant and therefore increase the characteristic impedance. Meanwhile, voids will also change the velocity of propagation in the transmission line.

3.5. Using an external sensor wire to detect corrosion

The characteristic impedance is very sensitive to the change of the radius a when the two conductors are close to each other according to equation (19). However, it may be very hard to apply a wire in the concrete grout near the steel cable. For retrofit of existing bridges, a sensor wire can be placed outside the concrete grout as long as the wire is parallel to the steel cable and the distance d is not too large. This method is very easy to use. However,

the biggest disadvantage of the external sensor wire is that the TDR measurement is less sensitive, as we mentioned above. A comparison between an internal sensor wire and an external sensor wire is shown in Figure 8.

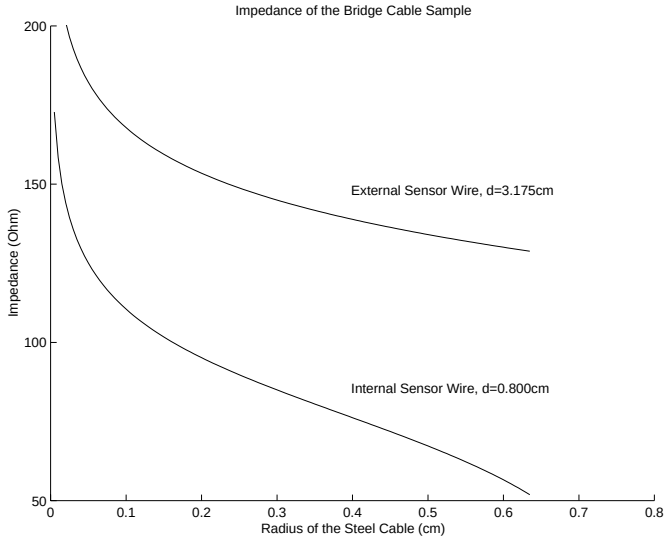

Figure 8. Characteristic impedance of bridge cable samples, where $b = 0.030cm$, and $a = 0.635cm$ if not corroded.

From Figure 8, for corrosion which reduces the radius from $0.635cm$ to $0.492cm$, the characteristic impedance will change from 51.9Ω to 68.0Ω if an internal sensor wire is applied. However, for an external sensor wire, the change of impedance is only $134.4\Omega - 128.8\Omega = 5.6\Omega$. Surface corrosion and small pitting corrosion may not be detectable under this circumstance. However, we also notice that there is no big difference between internal and external sensor wires if a is small. It means that the external sensor wire can be used to detect serious corrosion as well as the internal wire. This fact is of significance because of the many existing aging bridges for which the TDR method may be used to detect corrosion before failure results.

4. EXPERIMENTAL RESULTS

TDR measurements were made on several bridge cable sections to verify the mathematical model. The measurements can be made either using a pulse generator/oscilloscope combination or using a commercially available TDR tester.

Figure 9 shows the TDR returns from seven-strand steel cable samples. The steel cables are 3 foot long and 1/2 inch in diameter. Corrosion was simulated by cutting several strands. The damage was produced over a 3 inch length, 16.5 inches from the end of the sample. The first marker indicates the initial reflection from the front of sample, and the third marker indicates the reflection from the end of sample about $10ns$ later. The initial reflection is positive compared to the baseline before the peak, which shows that the characteristic impedance of the sample is larger than 50Ω. The impedance is measured as 56Ω. It is close to 52Ω, which is predicated by our model. Because the sample was terminated by a short circuit, the reflection from the end of the sample is negative. The second marker indicates the reflection from the corrosion site. Comparing Figure 9a and Figure 9b, we find that the magnitude of the reflection depends on the severity of the corrosion.

Figure 10 shows the TDR reflection from a 10 foot steel rebar sample. The sample has a 70% [‡] pitting corrosion 40 inches from the end of the sample and a 40% pitting corrosion 40 inches further down. The simulated pitting corrosion is a groove 1/2 inch wide. The two markers in Figure 10 indicate the pulse reflections from the corrosion sites. The reflections are small because the corrosion is occurred over a short length.

For the 3 foot sample with two broken strands, we found that the position of the sensor wire relative to the steel cable had a strong effect on the magnitude of the reflection as shown in Figure 11. The reflection is stronger when the sensor wire is close to the broken strand. This result is consistent with the theoretical analysis.

[‡] The percentage is the percentage reduction of the cross-sectional area at the corrosion site.

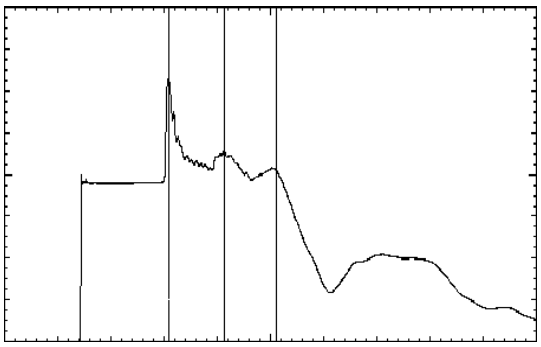

a. Six strands are broken at $1.5ft$

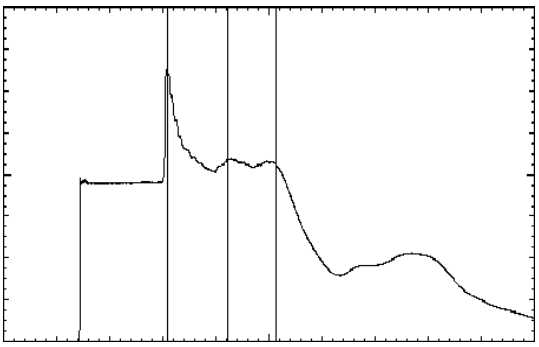

a. Two strands are broken at $1.5ft$

Figure 9. TDR returns from 3 foot seven-strand steel cable samples

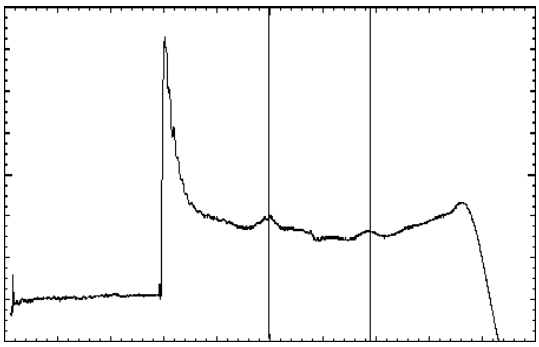

Figure 10. TDR returns from 10 foot steel rebar sample with 70% pitting corrosion at $3.3ft$ and 40% pitting corrosion at $6.6ft$.

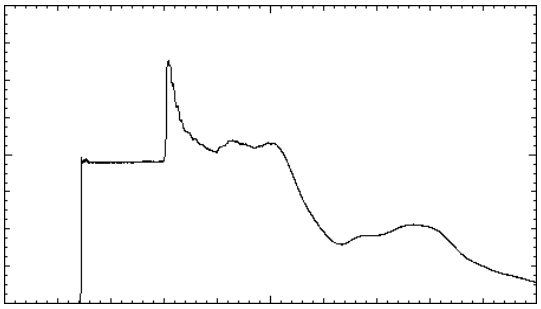

a. Sensor wire is next to the broken strands.

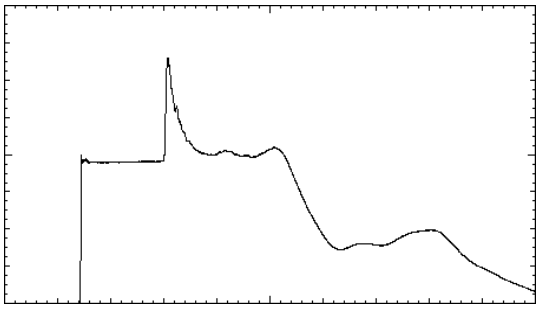

b. Sensor wire is close to the broken strands.

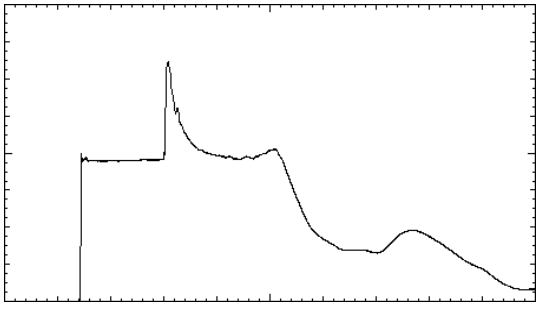

c. Sensor wire is at the opposite side from the broken strands.

Figure 11. TDR returns from 3 foot sample

As we stated in Section 2, the system risetime T_r is an important factor which determines whether or not a small mismatch can be detected. We made TDR measurements on a 3 foot seven-strand cable sample with risetimes varying from $500ps$ to $3ns$. When T_r is greater than $2ns$, the 3 inch long breakage of two strands is not detectable as shown in Figure 12.

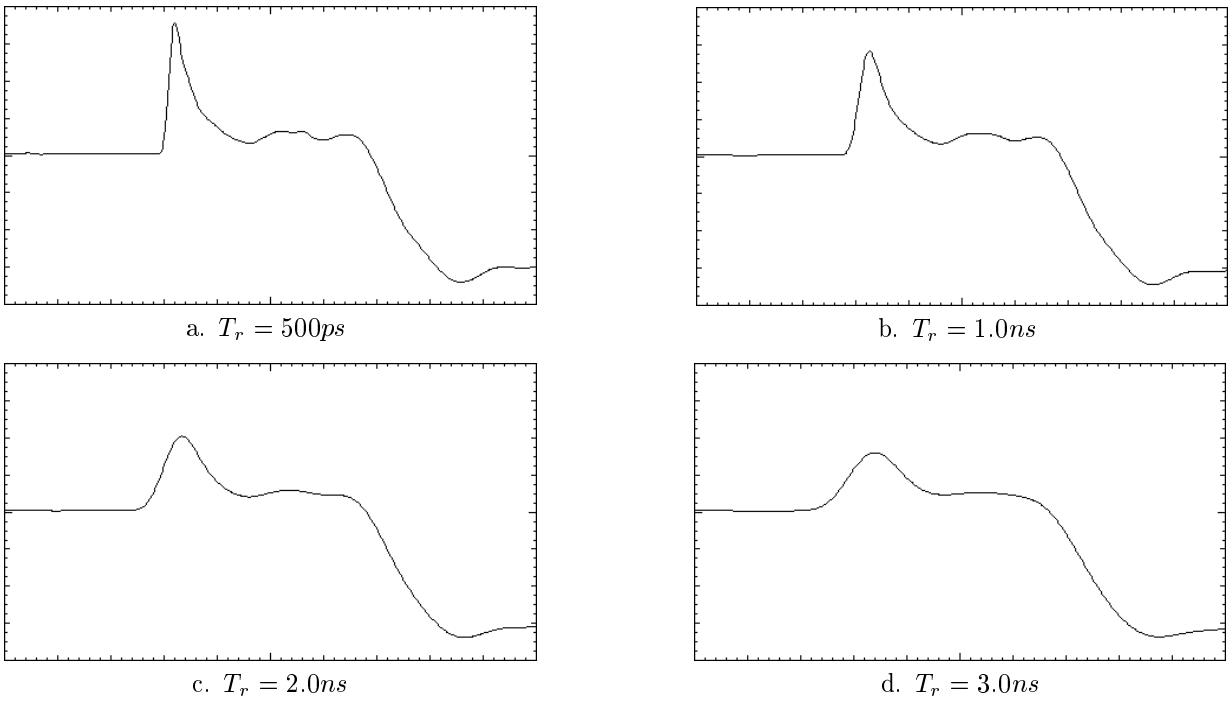

a. $T_r = 500ps$ b. $T_r = 1.0ns$

c. $T_r = 2.0ns$ d. $T_r = 3.0ns$

Figure 12. Comparison of TDR returns with different risetime T_r. The sample is 3 foot long and has two broken strands at $1.5ft$.

5. NOISE IN THE MEASUREMENT

In the TDR measurements of bridge cables in real structures, strong noise signals may be present. An example is shown in Figure 13. It is the TDR reflection from a 60 foot steel rebar sample. The sample has a 2 inch long, 50% pitting corrosion 36 feet from the end of the sample. The reflection from the corrosion site is indicated with the small arrow. It is identifiable but is only slightly larger than the noise signal.

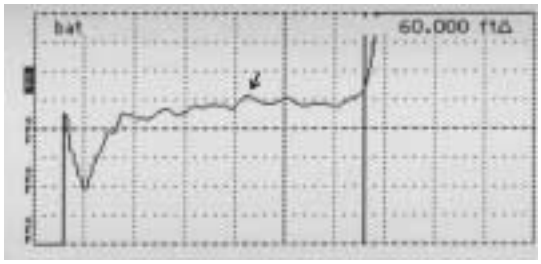

Figure 13. TDR return from a 60 foot steel rebar with a 50% pitting corrosion at $36ft$

The issue of noise is the focus of ongoing research. For random noise, we can repeat the measurements and average the results to remove the noise. In the TDR tests of long samples, some of the noise is repeatable. We expect this kind of noise in real structures because the steel components near the cable under test will definitely disturb the electric field. Variations of d, the distance between the steel cable and the sensing wire, will also cause undesirable noise. However, as long as the relative positions of these conductors do not change, the noise will remain the same.

If we make several TDR tests for the same cable over a long time period, the later TDR results should be identical to the former ones except for the corrosion sites. A differential comparison of stored signals with newly measured ones can cancel the effect of noise and reveal corrosion that occurred between the time of the two measurements.

6. CONCLUSIONS

Time domain reflectometry can be effectively used as a nondestructive evaluation technique for corrosion detection of embedded or encased steel cables. By applying a sensor wire alongside the bridge cable, we can model the cable as an asymmetric, twin-conductor transmission line. The distributed parameters of the transmission line can be calculated from the geometry and material parameters of the cable. Physical defects of the bridge cable, such as abrupt pitting corrosion, general surface corrosion, and voids in the concrete grout, will change the electromagnetic properties of the line. These defects can be modeled as different kinds of discontinuities. An abrupt pitting corrosion will cause a positive reflection, while a general surface corrosion causes greater energy loss. Voids in concrete will change the dielectric constant of the system and therefore change the impedance. All of these effects can be detected by TDR. In new bridges, an insulated sensing wire can be embedded in the concrete grout with the steel cable for a better accuracy. External sensing wires applied outside of the protective sheathing also can be used for already existing bridges, but with reduced measurement sensitivity. We verified our model by measurements made on fabricated bridge cable sections with built-in defects, and were able to detect the defects with TDR. This nondestructive evaluation technique can also be applied to other steel reinforced structures.

ACKNOWLEDGMENTS

This work was supported in part by the National Science Foundation under grant CMS-9700164 and the Delaware Transportation Institute under grant No.929.

REFERENCES

1. B. Wietek and E. Kunz, "Permanent corrosion monitoring for reinforced and prestressed concrete structures," in *Proceedings of IABSE Symposium*, (San Francisco, CA), 1995.
2. F. A. Zahn and B. Bitterli, "Developments in non-destructive stay cable inspection methods," in *Proceedings of IABSE Symposium*, pp. 861–866, (San Francisco, CA), 1995.
3. "Time domain refectometry theory," *Hewlett-Packard Application Note 1304-2* , 1988.
4. J. R. Andrews, "Time domain refectometry," in *Proceedings, Symposium on Time Domain Reflectometry in Environmental, Infrastructure, and Mining Applications*, (Evanston, IL), 1994.
5. R. Cole, "Time-domain spectroscopy of dielectric materials," *IEEE Tran.* **IM25**, pp. 371–375, 1976.
6. S. K. Bhatia, R. G. Hunsperger, and M. J. Chajes, "Modeling electromagnetic properties of bridge cables for non-destructive evaluation," in *Proceedings of International Conference on Corrosion and Rehabilitation of Reinforced Concrete Structures*, (Orlando, FL), 1998.
7. N. Rao, *Elements of Engineering Electromagnetics, 3rd ed*, Prentice-Hall, 1991.
8. W. Liu, "Nondestructive evaluation of bridge cables using time domain refectometry," Master's thesis, University of Delaware, 1998.